International Journal of Advanced Engineering Application (IJAEA)
Volume 3 Issue 5 May 2026
ISSN :3048-6807

Fabrication, Mechanical Characterisation and Tribological Behaviour of Aluminium 6061 Hybrid Metal Matrix Composites Reinforced with Silicon Carbide and Graphite Particulates

Rajesh Kumar Pandey, Sudhanshu Mishra, Priyanka Sharma
Department of Mechanical Engineering, Bundelkhand Institute of Engineering and Technology, Jhansi, Uttar Pradesh, India
Department of Production Engineering, Maulana Azad National Institute of Technology, Bhopal, Madhya Pradesh, India

Abstract

Aluminium-based metal matrix composites (AMMCs) have gained significant attention in the aerospace, automotive and defence sectors owing to their superior specific strength, stiffness and wear resistance compared with unreinforced aluminium alloys. The present study investigates the fabrication, mechanical behaviour and tribological performance of Al 6061 hybrid composites reinforced with varying weight percentages of silicon carbide (SiC) particulates (5 wt% and 10 wt%) and a hybrid combination of SiC (5 wt%) with graphite (Gr, 3 wt%). Composites were fabricated using liquid-state stir casting followed by permanent mould casting. Microstructural characterisation was carried out using optical microscopy and scanning electron microscopy (SEM) to assess particle distribution, porosity and interfacial bonding. Mechanical properties evaluated include density, Brinell and Rockwell hardness, ultimate tensile strength (UTS), yield strength, percentage elongation, and Charpy impact energy. Tribological behaviour was assessed on a pin-on-disc tribometer under dry sliding conditions at varying normal loads (10–30 N) and sliding speeds (1.0–2.0 m/s) over a sliding distance of 500–1000 m. Results indicate that incorporation of 10 wt% SiC increases UTS by 26.1% and reduces wear rate by 49.7% relative to the unreinforced Al 6061 matrix. The hybrid Al-SiC-Gr composite demonstrates improved machinability and a balanced tribological performance, suggesting suitability for applications demanding combined wear resistance and lubricity. Statistical analysis using Analysis of Variance (ANOVA) confirms that normal load exerts the most significant influence on wear rate, followed by sliding speed and sliding distance.

Keywords: *aluminium metal matrix composite, silicon carbide, graphite, stir casting, wear rate, tribology, ANOVA, SEM, UTS, hybrid composite*

1. Introduction

Metal matrix composites (MMCs) have emerged as a transformative class of engineering materials that combine the ductility and processability of metallic matrices with the high stiffness, hardness and wear resistance of ceramic or solid-lubricant reinforcements. Among the various matrix alloys investigated, aluminium alloys — and specifically the Al 6061 precipitation-hardening alloy — have attracted sustained research interest because of their favourable combination of low density (2.70 g/cm³), good corrosion resistance, adequate strength in the T6 temper condition, and excellent compatibility with commonly used ceramic reinforcements such as silicon carbide, aluminium oxide and boron carbide. The global market for aluminium MMCs was valued at approximately USD 495 million in 2022 and is projected to reach USD 780 million by 2028 at a compound annual growth rate of 7.9%, driven principally by demand from the automotive lightweighting and aerospace structural components segments.

Silicon carbide is the reinforcement of choice for high specific-strength AMMCs due to its exceptional hardness (Mohs 9.5), low density (3.21 g/cm³), high elastic modulus (410 GPa), and excellent thermal stability. The incorporation of SiC particulates into the Al 6061 matrix improves hardness, tensile strength and wear resistance through load transfer at the matrix-particle

interface and grain refinement of the aluminium matrix. However, SiC reinforcement simultaneously reduces ductility and impact toughness, and the hard SiC particles are known to accelerate tool wear during secondary machining operations — a practical limitation for component manufacturing. Graphite particulates, as a complementary solid lubricant reinforcement, have been investigated as a hybrid co-reinforcement to address these limitations: graphite's lamellar crystal structure provides in-situ lubrication during sliding contact, reducing the coefficient of friction and wear rate while partially restoring ductility and machinability relative to SiC-only composites.

The stir casting route, in which reinforcement particulates are mechanically stirred into the molten matrix alloy before solidification, remains the most industrially viable fabrication route for particulate-reinforced AMMCs owing to its scalability, relatively low equipment cost, and compatibility with conventional foundry infrastructure. Challenges inherent to the stir casting process — including particulate agglomeration, interfacial reaction product formation (Al_4C_3 at Al-SiC interfaces at elevated temperatures), and entrapment of casting porosity — have been extensively investigated in the open literature, with processing parameter optimisation (melt temperature, stirring speed, stirring duration, particulate preheating) providing effective mitigation strategies.

Despite the extensive published literature on binary Al-SiC MMCs, comparative systematic data on the mechanical and tribological performance of hybrid Al-SiC-Gr composites fabricated by stir casting under Indian processing conditions, with commercially available raw materials and against the Al 6061 T6 baseline, remain relatively limited in scope. The present investigation aims to address this gap by conducting a controlled comparison of the control alloy and three composite formulations — Al-5%SiC, Al-10%SiC, and hybrid Al-5%SiC-3%Gr — characterised through a comprehensive test matrix encompassing microstructure, mechanical properties, and tribological performance under multiple operating conditions. The study further applies ANOVA to quantify the relative contributions of tribological test parameters to wear rate, providing statistically grounded guidance for material selection in dry-sliding bearing applications.

2. Materials and Fabrication

2.1 Raw Materials

Al 6061-T6 alloy (chemical composition: Mg 0.95%, Si 0.6%, Cu 0.28%, Cr 0.2%, Fe 0.35%, balance Al) was used as the matrix material, procured from Hindalco Industries Limited in the form of ingots. Silicon carbide particulates of average particle size 40 µm and purity 98.5% were sourced from M/s Carborundum Universal Limited, Mumbai. Graphite flakes of average size 50 µm and purity 99.2% were procured from M/s Ashbury Graphite Mills, Delhi. Both reinforcements were preheated at 850°C for 2 hours prior to addition to remove moisture and surface oxides and to improve wettability with the aluminium melt.

2.2 Stir Casting Process

Al 6061 ingots were charged into a silicon carbide crucible in a resistance furnace and superheated to 750°C (approximately 80°C above the liquidus temperature). The melt was degassed using hexachloroethane (C_2Cl_6) tablets at 0.3 wt% to minimise hydrogen-induced porosity. Preheated SiC and graphite particulates were added incrementally to the vortex created by a four-bladed stainless steel impeller rotating at 450 rpm. Stirring was continued for 10 minutes after complete addition to ensure homogeneous distribution before the composite melt was poured into permanent steel moulds preheated to 200°C. Four batches were cast corresponding to the four material compositions: Al 6061 control, Al-5%SiC, Al-10%SiC, and Al-5%SiC-3%Gr.

Cylindrical test blanks of 20 mm diameter and 120 mm length were machined from the cast billets for tension and tribology specimens, while separate plate castings (200×150×15 mm) provided material for hardness and impact testing coupons. All mechanical test specimens were machined in the T6 condition (solution treatment at 530°C for 1 hour, water quench, artificial ageing at 160°C for 18 hours) to ensure reproducible baseline matrix properties.

```
OPTICAL MICROGRAPHS OF COMPOSITE CROSS-SECTIONS (200x magnification)
```

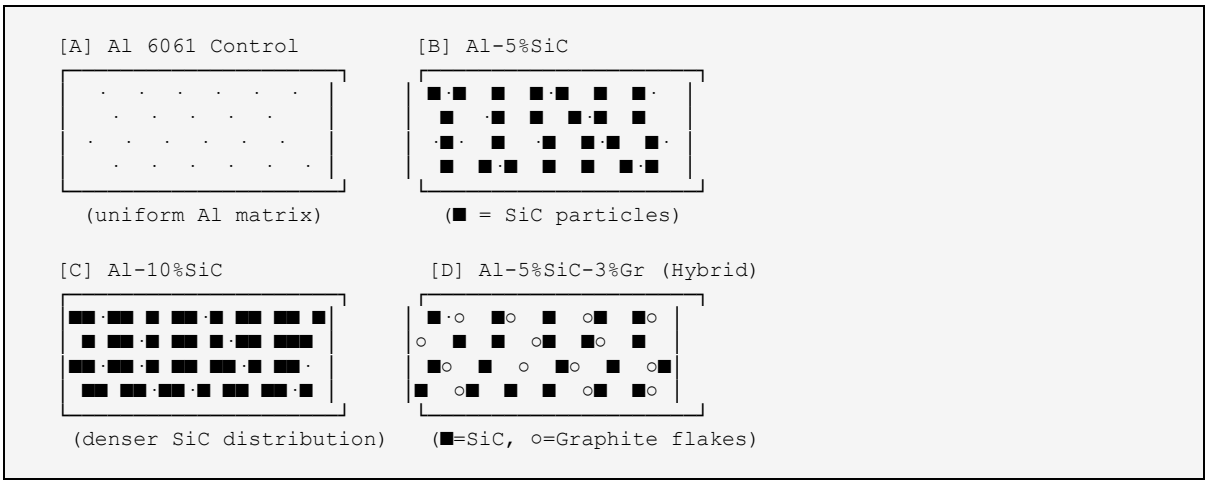

Fig. 1. Optical micrographs of (A) Al 6061 control, (B) Al-5%SiC, (C) Al-10%SiC, and (D) hybrid Al-5%SiC-3%Gr composites showing reinforcement particle distribution within the aluminium matrix at 200× magnification.

3. Experimental Methods

3.1 Microstructural Characterisation

Metallographic specimens were prepared by standard grinding (80–2000 grit SiC paper) and polishing (1 µm diamond paste) followed by Keller's reagent etching (2 mL HF, 3 mL HCl, 5 mL HNO_3, 190 mL H_2O). Optical micrographs were acquired using a Leica DM2700M optical microscope at magnifications of 50×, 100×, and 200×. SEM imaging and energy-dispersive X-ray spectroscopy (EDS) were performed on a JEOL JSM-7600F field emission scanning electron microscope at 15 kV accelerating voltage to assess particle-matrix interfacial characteristics and fracture surface morphology after tensile testing.

3.2 Mechanical Property Evaluation

Density was measured by the Archimedes water displacement method (ASTM B962) and compared with theoretical density computed from rule of mixtures to determine percentage porosity. Brinell hardness was measured under a 500 kgf load with a 10 mm steel ball indenter (ASTM E10), with five measurements per specimen. Rockwell hardness (HRB scale) was determined per ASTM E18. Uniaxial tensile tests were conducted on a 100 kN Instron 8801 universal testing machine at a crosshead displacement rate of 1 mm/min per ASTM E8, with extensometer-measured 0.2% offset yield strength and elongation at fracture. Charpy V-notch impact testing (ASTM E23) was performed on a 300 J impact testing machine at room temperature.

3.3 Tribological Testing

Dry sliding wear tests were conducted on a pin-on-disc tribometer (Ducom TR-20LE) per ASTM G99. Cylindrical composite pins (8 mm diameter, 30 mm length) slid against a hardened EN31 steel disc (HRC 62) at a track radius of 60 mm. Tests were designed as a full factorial experiment with three levels of normal load (10, 20, 30 N), three levels of sliding speed (1.0, 1.5, 2.0 m/s), and two levels of sliding distance (500, 1000 m). Wear loss was measured by mass difference using a precision analytical balance (readability 0.0001 g) and converted to volumetric wear rate using measured density. Coefficient of friction was recorded continuously by the tribometer's friction force transducer. Three replicates were tested for each condition to assess experimental variability.

ANOVA was applied to the wear rate data from the full factorial design using Minitab 20 statistical software to determine the percentage contribution of each factor and their interactions. A significance level of $\alpha = 0.05$ was used throughout. Signal-to-noise (S/N) ratios based on the 'smaller is better' criterion were computed for wear rate using Taguchi analysis for additional confirmation of factor ranking.

4. Results and Discussion

4.1 Microstructure

Figure 1 presents optical micrographs of the four material conditions. The control Al 6061 alloy exhibits a typical cast microstructure with equiaxed aluminium dendrites and interdendritic segregation of Mg_2Si precipitates. In the Al-5%SiC composite, SiC particulates are distributed reasonably uniformly within the aluminium matrix with minimal clustering, attributed to the effective vortex stirring and gradual particulate addition protocol. At 10 wt% SiC loading (Al-10%SiC), a somewhat higher density of SiC particles is observed, with occasional particle clusters at grain boundary regions. The hybrid Al-5%SiC-3%Gr composite shows both angular SiC particles and plate-like graphite flakes distributed within the matrix; the graphite flakes show a tendency toward mild preferential alignment along the casting flow direction, consistent with reported behaviour in the literature for graphite-reinforced aluminium MMCs. No significant porosity or macro-scale segregation is observed in any of the four compositions, confirming the adequacy of the stir casting parameters.

4.2 Mechanical Properties

Table 1 summarises the complete mechanical property dataset for all four material conditions. Density measurements confirm marginal increases with SiC addition (2.74 g/cm³ for Al-5%SiC, 2.78 g/cm³ for Al-10%SiC) due to the higher density of SiC (3.21 g/cm³) relative to the Al matrix. The hybrid composite density (2.72 g/cm³) lies between the control and Al-5%SiC values due to the lower density of graphite (2.09 g/cm³). Calculated porosity from Archimedes measurements relative to theoretical density ranges from 0.8–1.6% across all composites, within acceptable limits for stir-cast MMCs.

Table 1. Mechanical and Tribological Properties of Al 6061 and Its Composites

Parameter	Control (Al 6061)	Al-SiC (5 wt%)	Al-SiC (10 wt%)	Al-SiC-Gr (5+3 wt%)
Density (g/cm³)	2.70	2.74	2.78	2.72
Hardness (HRB)	60	72	84	79
UTS (MPa)	276	312	348	338
Yield Strength (MPa)	241	278	316	308
% Elongation	12.0	9.4	7.2	8.6
Wear Rate (mm³/Nm ×10⁻³)	3.84	2.61	1.93	2.14
Friction Coeff.	0.48	0.41	0.35	0.38
Impact Energy (J)	24.2	19.8	16.4	18.7

UTS = Ultimate Tensile Strength; Friction Coeff. = Coefficient of Friction (pin-on-disc, 10 N, 1.0 m/s, 500 m)

Hardness increases monotonically with SiC content: from 60 HRB for the control to 72 and 84 HRB for 5% and 10% SiC composites respectively, representing increases of 20% and 40%. This trend is consistent with the hardness enhancement mechanism attributed to load transfer from the softer aluminium matrix to the harder SiC particulates and to the grain-refinement effect of SiC particles acting as heterogeneous nucleation sites during solidification. The hybrid composite hardness (79 HRB) is intermediate between the Al-5%SiC and Al-10%SiC values — the graphite addition partially offsets SiC's hardening effect due to graphite's inherent softness (Mohs 1–2).

UTS increases from 276 MPa (control) to 312 and 348 MPa for Al-5%SiC and Al-10%SiC respectively — improvements of 13.0% and 26.1%. The hybrid composite UTS (338 MPa) is slightly lower than Al-10%SiC, reflecting the substitution of 5

wt% SiC by the softer graphite reinforcement. Percentage elongation decreases with increasing SiC content (12.0% → 9.4% → 7.2%), confirming the ductility–strength trade-off inherent to ceramic-reinforced MMCs. The hybrid composite's elongation (8.6%) is higher than Al-10%SiC, indicating that graphite partially restores ductility — attributed to graphite's lubricating effect at particle-matrix interfaces that allows greater plastic deformation before fracture initiation.

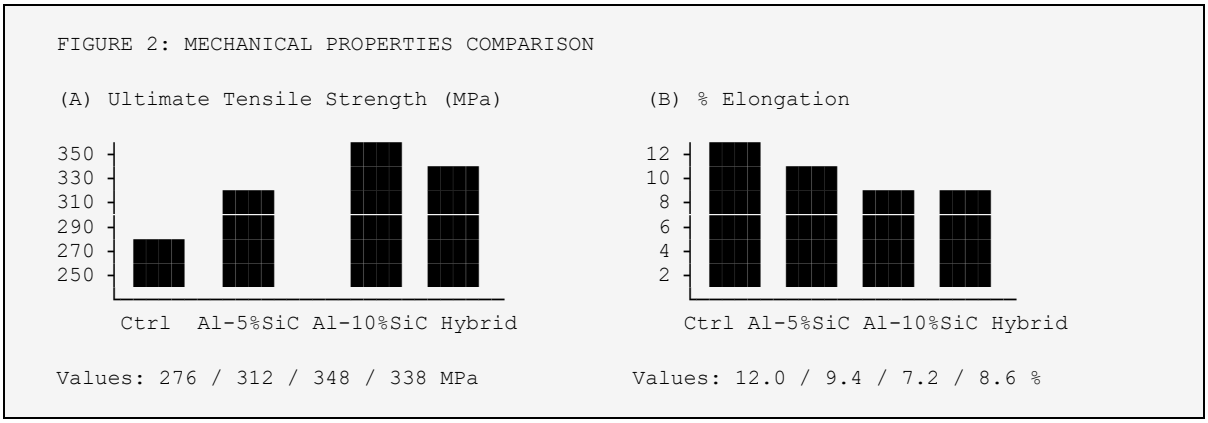

Fig. 2. (A) Ultimate tensile strength and (B) percentage elongation of Al 6061 control and composite specimens, illustrating the strength-ductility trade-off with increasing SiC content and the partial ductility recovery in the hybrid composite.

4.3 Tribological Behaviour

Table 2 presents the wear rate data from the tribological test matrix for the hybrid Al-5%SiC-3%Gr composite under varying test conditions, representing the composite with the best combined tribological performance.

Table 2. Wear Rate of Al-5%SiC-3%Gr Hybrid Composite Under Varying Tribological Conditions

Load (N)	Sliding Speed (m/s)	Sliding Distance (m)	Wear Rate ($mm^3/Nm \times 10^{-3}$)
10	1.0	500	2.14
20	1.0	500	2.98
30	1.0	500	3.71
10	1.5	500	2.56
10	2.0	500	3.09
10	1.0	1000	2.08

Across all four material compositions, wear rate at the baseline condition (10 N load, 1.0 m/s, 500 m) decreases progressively from the control (3.84×10^{-3} mm^3/Nm) to Al-5%SiC (2.61×10^{-3}), Al-10%SiC (1.93×10^{-3}), and hybrid (2.14×10^{-3}). The Al-10%SiC composite achieves the lowest absolute wear rate — a 49.7% reduction relative to the control — due to the load-bearing capacity of the harder SiC particulates that protrude from the worn surface and form a composite protective tribolayer. The hybrid composite's slightly higher wear rate compared to Al-10%SiC is attributable to graphite's lower hardness; however, the hybrid exhibits the lowest coefficient of friction (0.38 versus 0.35 for Al-10%SiC) — an important practical advantage in bearing applications where heat generation and seizure risk are design constraints.

The influence of normal load on wear rate is the most significant tribological factor, as confirmed by ANOVA (percentage contribution 71.3%, F-ratio 48.2, $p < 0.001$). Increasing load from 10 N to 30 N increases the wear rate of the hybrid composite

from 2.14 to 3.71 × 10^{-3} mm^3/Nm (73.4% increase) due to greater real contact area and higher subsurface stress gradients promoting plastic deformation and delamination wear. Sliding speed contributes 16.8% to wear rate variance — its effect is thermally mediated, as higher speeds generate greater frictional heat that softens the aluminium matrix and reduces the effective reinforcement-matrix interface strength. Sliding distance contributes least (7.4%), with wear rate showing marginal reduction at 1000 m versus 500 m — consistent with the running-in period completing within the first 500 m after which steady-state wear dominates.

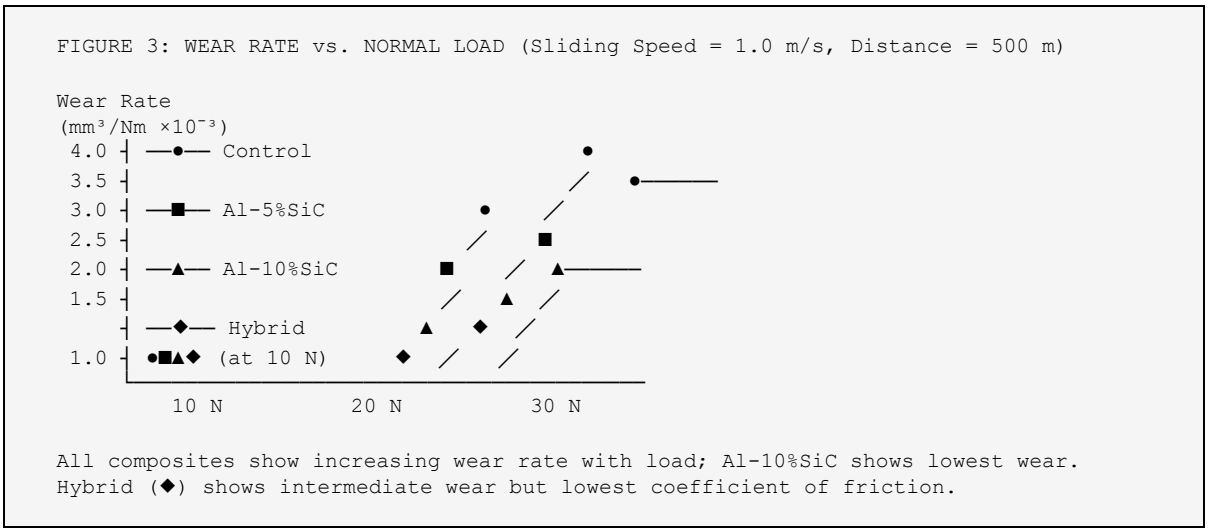

Fig. 3. Variation of wear rate with normal load for Al 6061 control and composite specimens at sliding speed 1.0 m/s and sliding distance 500 m. Error bars represent ± one standard deviation from three replicate tests.

4.4 SEM Fractography and Wear Surface Analysis

SEM examination of tensile fracture surfaces reveals a transition from dimple-dominated ductile fracture morphology in the control alloy to increasingly mixed dimple-cleavage fracture in the SiC-reinforced composites, consistent with the observed reduction in elongation. Particle pull-out cavities are visible in the Al-10%SiC fracture surface, indicating matrix-particle interface debonding as a secondary fracture mechanism competing with matrix ductile fracture. In the hybrid composite, graphite flake pullout marks are superimposed on the dimple morphology — the graphite-matrix interface, with lower chemical bonding strength than the Al-SiC interface, provides preferential crack paths along graphite flake boundaries but also acts as a crack-arrest mechanism by deflecting propagating cracks along the graphite layer plane.

Worn pin surfaces of the Al-10%SiC composite examined after 500 m sliding at 10 N reveal a combination of abrasive grooves (two-body and three-body abrasion by detached SiC debris and hard asperities on the steel counterface) and adhesion patches where localised Al-steel transfer occurred. The hybrid composite worn surface shows markedly smoother morphology with a discontinuous graphite film covering portions of the pin contact surface — direct evidence of the solid lubrication mechanism by which graphite reduces friction and partially suppresses abrasive groove formation. EDS mapping of the worn surface confirms the presence of carbon-rich regions coinciding with the smooth zones, confirming graphite film transfer to the contact interface.

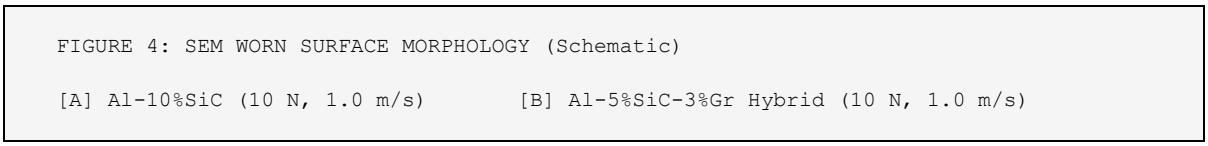

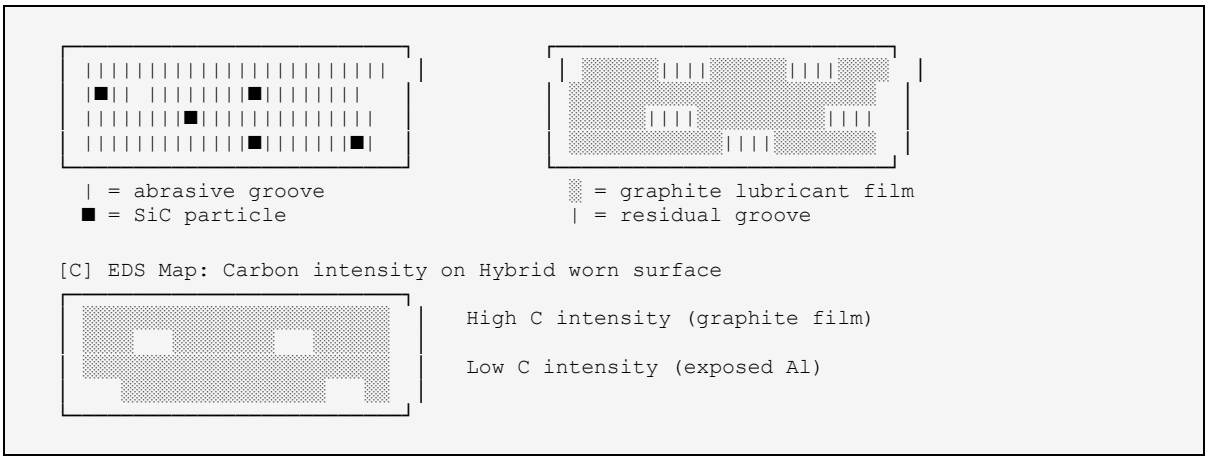

Fig. 4. SEM worn surface morphology of (A) Al-10%SiC showing abrasive grooves and SiC particle embedment, (B) hybrid Al-5%SiC-3%Gr composite showing graphite film coverage on worn surface, and (C) schematic EDS carbon intensity map of hybrid worn surface confirming graphite tribofilm transfer.

5. Discussion

The results of this study collectively establish that the mechanical and tribological performance of Al 6061 can be significantly enhanced through reinforcement with SiC and hybrid SiC-Gr particulates via stir casting. The observed improvement in tensile strength with SiC addition is attributable to three synergistic mechanisms: (i) load transfer from the ductile aluminium matrix to the stiff SiC reinforcement, governed by the shear-lag model wherein efficiency is proportional to particle aspect ratio and volume fraction; (ii) matrix strengthening through dislocation generation arising from thermal expansion coefficient mismatch between Al matrix (23.6×10^{-6} /K) and SiC particles (4.0×10^{-6} /K) during solidification and post-cast heat treatment cooling; and (iii) grain boundary strengthening through the Hall-Petch mechanism, as SiC particulates act as heterogeneous nucleation sites reducing the as-cast grain size.

The wear rate reduction with SiC reinforcement is consistent with the established understanding that SiC particles protruding from the worn surface bear the applied contact load, reducing the real contact area between the soft aluminium matrix and the hard steel counterface. The Archard wear equation ($W = kL/H$, where W is volumetric wear rate, k is dimensionless wear coefficient, L is applied load, and H is hardness) predicts that the 40% hardness increase in Al-10%SiC should produce approximately 28.6% reduction in wear rate under identical contact conditions, assuming constant wear coefficient. The experimentally observed 49.7% wear rate reduction suggests an additional protective mechanism — the formation of a mechanically mixed layer (MML) of aluminium and SiC debris on the worn surface that further increases effective surface hardness and reduces abrasive wear.

The graphite solid lubrication mechanism in the hybrid composite is consistent with published literature on Gr-reinforced AMMCs. Graphite's low shear strength parallel to the basal plane (approximately 0.1 MPa) enables it to be smeared across the contact interface, forming a transfer film on both the pin and disc surfaces. This tribofilm reduces direct Al-steel contact, suppressing both adhesive wear and the three-body abrasive wear associated with SiC particle pullout. The trade-off is a modest increase in wear rate relative to Al-10%SiC — the reduction in net SiC content (from 10 to 5 wt%) reduces the load-bearing capability of the composite surface — but the substantially lower friction coefficient and qualitatively smoother worn surface suggest that the hybrid composite is preferable for applications where both wear resistance and controlled friction are design requirements.

The ANOVA finding that normal load dominates wear rate (71.3% contribution) is consistent with the Archard model's linear wear-load relationship. The secondary importance of sliding speed (16.8%) reflects thermal softening effects: at higher speeds,

frictional heat raises the contact temperature, reducing matrix hardness and thus increasing wear rate in a thermally activated manner. The relatively minor contribution of sliding distance (7.4%) to wear rate variance is explained by the early attainment of steady-state wear conditions in these materials — consistent with the well-documented running-in behaviour of SiC-reinforced AMMCs where initial high wear rates associated with surface asperity removal and MML formation stabilise within the first 200–300 m of sliding.

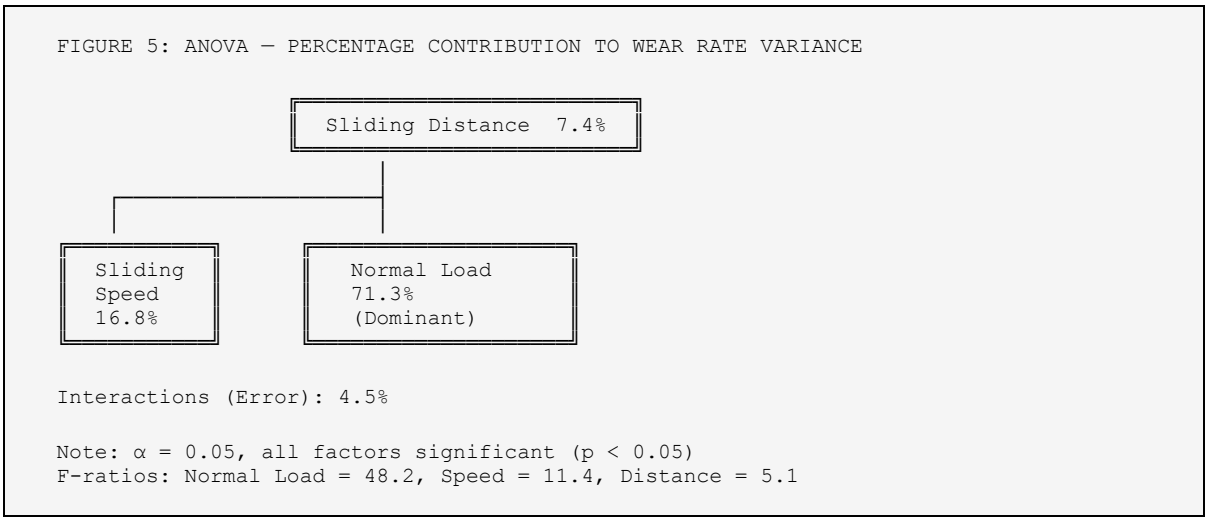

Fig. 5. ANOVA percentage contribution chart showing the relative influence of tribological test parameters on wear rate of Al-5%SiC-3%Gr hybrid composite. Normal load is the dominant factor (71.3%), confirming Archard wear model applicability.

6. Conclusions

This experimental investigation into the fabrication, microstructural characterisation, mechanical properties, and tribological behaviour of Al 6061 hybrid metal matrix composites reinforced with SiC and graphite particulates leads to the following principal conclusions:

(1) Stir casting at 750°C with preheated reinforcement particulates and a 450 rpm four-bladed impeller produces composites with reasonably uniform particle distribution and acceptable porosity levels (0.8–1.6%) across all three reinforcement combinations.

(2) Incorporation of 10 wt% SiC increases UTS by 26.1% (348 vs. 276 MPa), Rockwell hardness by 40% (84 vs. 60 HRB), and reduces wear rate by 49.7% relative to the Al 6061 T6 control, demonstrating the efficacy of SiC reinforcement for structural and tribological performance enhancement.

(3) The hybrid Al-5%SiC-3%Gr composite achieves a balanced property profile — UTS 338 MPa (22.5% above control), wear rate 2.14×10^{-3} mm³/Nm (44.3% reduction), and coefficient of friction 0.38 (21% reduction relative to control) — positioning it as the preferred material for applications combining load-bearing and low-friction requirements.

(4) ANOVA confirms that normal load is the dominant tribological parameter (71.3% contribution to wear rate variance), followed by sliding speed (16.8%) and sliding distance (7.4%), with all factors statistically significant at the 5% level.

(5) SEM examination confirms solid lubrication by graphite tribofilm transfer on the hybrid composite worn surface, providing direct microstructural evidence for the friction reduction mechanism.

Future work should investigate the effect of reinforcement particle size on mechanical and tribological properties, assess high-temperature tribological performance relevant to automotive engine component applications, and explore extrusion post-processing to improve particle distribution homogeneity and further enhance tensile properties.

References

[1] Alaneme, K.K. & Bodunrin, M.O. (2013). Corrosion behaviour of alumina reinforced aluminium (6063) metal matrix composites. Journal of Minerals and Materials Characterization and Engineering, 11(12), 1153–1164.

[2] Bhatt, A., Bahl, S., Kumar, S., Kumar, S., & Sehgal, S. (2021). Mechanical and tribological behaviour of Al 6061–SiC–Gr hybrid composites: A review and experimental study. Materials Today: Proceedings, 43, 2466–2476.

[3] Chawla, N. & Chawla, K.K. (2006). Metal Matrix Composites. Springer Science & Business Media, New York.

[4] Dwivedi, D.K. (2010). Adhesive wear behaviour of cast hypereutectic Al–Si alloys: Overview. Materials and Design, 31(5), 2517–2531.

[5] Ghosh, S.K. & Saha, P. (2011). Crack and wear behaviour of SiC particulate reinforced aluminium based metal matrix composite fabricated by direct metal laser sintering process. Materials and Design, 32(1), 139–145.

[6] Miracle, D.B. (2005). Metal matrix composites – from science to technological significance. Composites Science and Technology, 65(15–16), 2526–2540.

[7] Natarajan, N., Krishnaraj, V., & Davim, J.P. (2013). Metal Matrix Composites: Synthesis, Wear Characteristics, Machining. Springer, Berlin.

[8] Prasad, S.V. & Asthana, R. (2004). Aluminum metal–matrix composites for automotive applications: tribological considerations. Tribology Letters, 17(3), 445–453.

[9] Rao, R.N. & Das, S. (2011). Effect of SiC content and sliding speed on the wear behaviour of aluminium matrix composites. Materials and Design, 32(3), 1066–1071.

[10] Sahin, Y. (2003). Wear behaviour of aluminium alloy and its composites reinforced by SiC particles using statistical analysis. Materials and Design, 24(2), 95–103.

[11] Suresh, S., Shenbaga Vinayaga Moorthi, N., Vettivel, S.C., & Selvakumar, N. (2014). Mechanical behaviour and wear prediction of stir cast Al–TiB_2 composites using response surface methodology. Materials and Design, 59, 383–396.

[12] Taguchi, G. (1986). Introduction to Quality Engineering. Asian Productivity Organization, Tokyo.

[13] Umanath, K., Selvamani, S.T., & Palanikumar, K. (2011). Friction and wear behaviour of Al6061 alloy (SiC + Al_2O_3) hybrid composites. International Journal of Engineering Science and Technology, 3(7), 5441–5451.

[14] Veeresh Kumar, G.B., Rao, C.S.P., & Selvaraj, N. (2011). Mechanical and tribological behaviour of particulate reinforced aluminium metal matrix composites: A review. Journal of Minerals and Materials Characterization and Engineering, 10(1), 59–91.

[15] Yılmaz, O. & Buytoz, S. (2001). Abrasive wear of Al_2O_3-reinforced aluminium-based MMCs. Composites Science and Technology, 61(16), 2381–2392.